ACCOUNTS
of chemical research

Photophysics of Individual Single-Walled Carbon Nanotubes

LISA J. CARLSON AND TODD D. KRAUSS*
Department of Chemistry, University of Rochester, Rochester, New York 14627

RECEIVED ON JUNE 2, 2007

CONSPECTUS

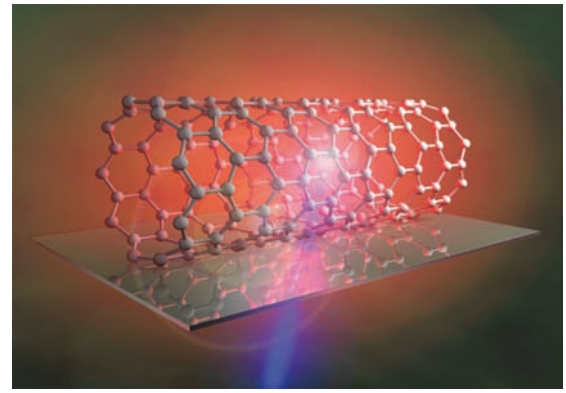

Single-walled carbon nanotubes (SWNTs) are cylindrical graphitic molecules that have remained at the forefront of nanomaterials research since 1991, largely due to their exceptional and unusual mechanical, electrical, and optical properties. The motivation for understanding how nanotubes interact with light (i.e., SWNT photophysics) is both fundamental and applied. Individual nanotubes may someday be used as superior near-infrared fluorophores, biological tags and sensors, and components for ultrahigh-speed optical communications systems. Establishing an understanding of basic nanotube photophysics is intrinsically significant and should enable the rapid development of such innovations.

Unlike conventional molecules, carbon nanotubes are synthesized as heterogeneous samples, composed of molecules with different diameters, chiralities, and lengths. Because a nanotube can be either metallic or semiconducting depending on its particular molecular structure, SWNT samples are also mixtures of conductors and semiconductors. Early progress in understanding the optical characteristics of SWNTs was limited because nanotubes aggregate when synthesized, causing a mixing of the energy states of different nanotube structures. Recently, significant improvements in sample preparation have made it possible to isolate individual nanotubes, enabling many advances in characterizing their optical properties.

In this Account, single-molecule confocal microscopy and spectroscopy were implemented to study the fluorescence from individual nanotubes. Single-molecule measurements naturally circumvent the difficulties associated with SWNT sample inhomogeneities. Intrinsic SWNT photoluminescence has a simple narrow Lorentzian line shape and a polarization dependence, as expected for a one-dimensional system. Although the local environment heavily influences the optical transition wavelength and intensity, single nanotubes are exceptionally photostable. In fact, they have the unique characteristic that their single molecule fluorescence intensity remains constant over time; SWNTs do not "blink" or photobleach under ambient conditions.

In addition, transient absorption spectroscopy was used to examine the relaxation dynamics of photoexcited nanotubes and to elucidate the nature of the SWNT excited state. For metallic SWNTs, very fast initial recovery times (300–500 fs) corresponded to excited-state relaxation. For semiconducting SWNTs, an additional slower decay component was observed (50–100 ps) that corresponded to electron–hole recombination. As the excitation intensity was increased, multiple electron–hole pairs were generated in the SWNT; however, these e—h pairs annihilated each other completely in under 3 ps. Studying the dynamics of this annihilation process revealed the lifetimes for one, two, and three e—h pairs, which further confirmed that the photoexcitation of SWNTs produces not free electrons but rather one-dimensional bound electron–hole pairs (i.e., excitons).

In summary, nanotube photophysics is a rapidly developing area of nanomaterials research. Individual SWNTs exhibit robust and unexpectedly unwavering single-molecule fluorescence in the near-infrared, show fast relaxation dynamics, and generate excitons as their optical excited states. These fundamental discoveries should enable the development of novel devices based on the impressive photophysical properties of carbon nanotubes, especially in areas like biological imaging. Many facets of nanotube photophysics still need to be better understood, but SWNTs have already proven to be an excellent starting material for future nanophotonics applications.

Published on the Web 02/19/2008 www.pubs.acs.org/acr
10.1021/ar700136v CCC: $40.75

Introduction

Single-walled carbon nanotubes (SWNTs) are cylindrical molecules known for their unique mechanical, electrical, and optical traits, which result from the strength of the carbon−carbon bond and the effects of quantum confinement around a nanotube's circumference. Carbon nanotubes have a tensile strength 20 times that of steel, carry 1000 times more current density than copper wires, and transport charges down the nanotube without significant scattering.[1] Recently, nanotubes have been integrated into an array of innovative devices, including highly sensitive atomic force microscope probes,[2] near-infrared glucose[3] and biological sensors,[4,5] field effect transistors, and flat panel displays.[1,6] Carbon nanotubes also have the potential to significantly impact the fields of energy storage[7] and molecular electronics.[8−12]

A carbon nanotube can be pictured as a graphene sheet rolled into a cylinder, such that two lattice points coincide (Figure 1a). The starting and ending lattice points dictate both the diameter and chirality of the SWNT, which are characterized by the integers (*n*, *m*) (Figure 1b). The chiral vector ($\vec{C}_h$) connects these points and the chiral angle (θ) specifies the tilt between the hexagonal lattice and the radial axis of the nanotube ($0° \leq \theta \leq 30°$).[13]

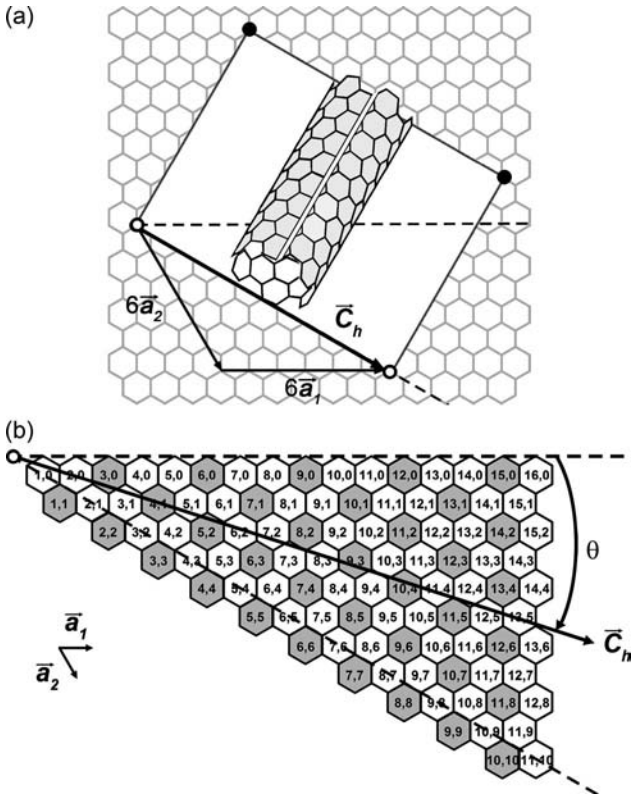

FIGURE 1. (a) Construction of a nanotube from a graphene sheet, where the white region represents the area used to form the nanotube. Two corresponding lattice points overlap (open or filled circles) to form a (6,6) nanotube with a chiral angle of 30°. (b) Depiction of possible SWNT (*n*, *m*) structures represented on a single graphene sheet. Semiconducting SWNTs are white and metallic SWNTs are shaded.

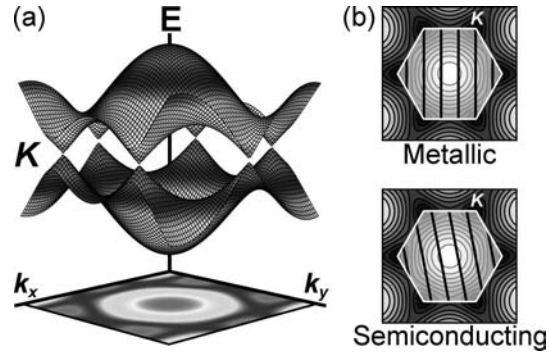

FIGURE 2. (a) Calculation of the 3D graphene energy band structure. A 2D contour shadow is projected onto the *xy* plane in reciprocal space. (b) Allowed electron states for nanotubes (solid black lines) pass through the *K*-point for metallic SWNTs but lie on either side of the *K*-point for semiconducting SWNTs.

$$\vec{C}_h = n\vec{a}_1 + m\vec{a}_2 \equiv (n, m) \quad (1)$$

$$\theta = \tan^{-1}[\sqrt{3}m/(2n + m)] \quad (2)$$

The nanotube energy band structure is also derived from graphene (a single sheet of graphite). A three-dimensional view of the graphene valence and conduction bands is shown in Figure 2a. Graphene is a semimetal because occupied π and unoccupied π^* energy bands overlap at six quantum states (called *K*-points); electrons in these states are free to conduct. For a semiconductor, however, occupied and unoccupied bands do not overlap, and an energy gap is produced. As illustrated in Figure 2b, the allowed electron states for a SWNT are a small subset of those in graphene, determined by the nanotube's diameter and twist (i.e., (*n*, *m*)).[14] One third of SWNTs are metallic because some of the allowed electron states intersect the conductive *K*-point [$(n - m) \bmod 3 \equiv 0$]. The rest are semiconducting because allowed electron states lie on either side of the *K*-point, creating an energy gap [$(n - m) \bmod 3 \equiv 1$ or 2].

The density of electronic states (DOS) indicates the number of allowed electron states at a particular energy and is useful for understanding optical transitions (Figure 3). The 0D DOS is discrete for small molecules that have well-defined energy levels. One-dimensional materials like carbon nanotubes display sharp peaks in the 1D DOS (called van Hove singularities) that are similar to molecular energy levels. In the simplest picture, optical transitions for SWNTs take place between matching peaks in the 1D DOS. These transitions are

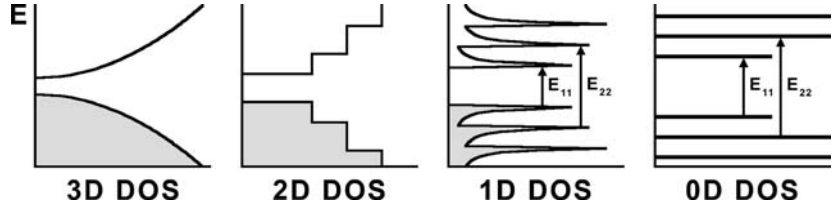

FIGURE 3. Diagram showing energy versus density of states for materials of various dimensions. Occupied electron energy levels (valence band) are shaded and unoccupied levels (conduction band) are white. The first two dipole-allowed absorption transitions (E_{11} and E_{22}) are labeled for the 0D and 1D densities of states.

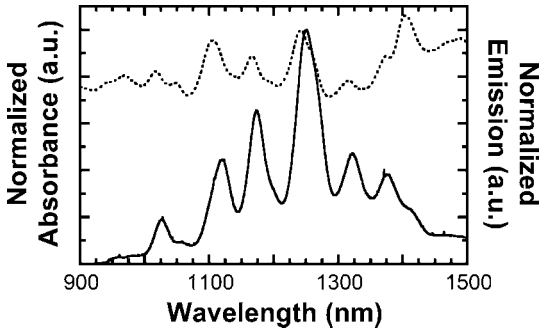

FIGURE 4. Spectra showing normalized absorbance (dotted) and fluorescence (solid) from an ensemble of HiPco-manufactured SWNTs suspended in SDS/D_2O. Resolved peaks correspond to various (*n*, *m*) structures.

abbreviated as E_{jj} (E_{11}, E_{22}, etc.).[15] The energy varies inversely with nanotube diameter according to

$$E_{jj} = 2ja_{C-C}\gamma_0/d_t \quad (3)$$

where j is the transition index, a_{C-C} is the nearest neighbor C−C distance, γ_0 is the nearest neighbor interaction energy, and d_t is the nanotube diameter.[13,16] However, accurate transition energies also depend on the (*n*, *m*) structure of the nanotube, partially due to the effects of sidewall curvature.[16]

Nanotubes aggregate when synthesized, thus limiting early optical studies to bundles of SWNTs. For bundles, the absorption spectrum exhibits severe inhomogeneous broadening as the result of mixing between the energy states of different nanotube structures.[17] Fluorescence is not observed from nanotube bundles because photoexcited carriers that are generated in semiconducting SWNTs relax along the efficient nonradiative channels provided by metallic SWNTs in the bundle.

Isolating individual nanotubes was a major advancement toward their optical characterization. O'Connell et al. pioneered a method to encapsulate SWNTs in a variety of surfactants including micelles,[18,19] polymers, and DNA.[20] Isolated semiconducting SWNTs fluoresce, revealing resolved optical transitions for distinct nanotube (*n*, *m*) structures (Figure 4).[18] To assign a specific (*n*, *m*) structure to each optical feature, the fluorescence energy and the diameter-dependent radial breathing mode (RBM) energy in the resonant Raman spectrum were correlated;[16] complicated fitting procedures were necessary because several assignments are plausible.[14,16] Spectral assignments were subsequently confirmed directly by single-molecule studies.[21]

Several qualitative features of the optical spectra of nanotubes are explained by a simple free electron picture of a SWNT excited state, but this model fails to accurately represent many experimental observations. For example, the free electron picture underestimates the energetic separation of the E_{11} electron states, while it both overestimates and underestimates E_{22} values.[22,23] Free electron models also predict that the ratio E_{22}/E_{11} should be 2, but its observed value is closer to 1.7 (i.e., the ratio problem).[14,24,25] These dissimilarities imply that electron−electron and electron−hole interactions strongly influence the physics underlying optical transitions.

Electrostatically bound electron−hole (e−h) pairs are known as excitons. In SWNTs, the electrostatic electron−hole interaction energy (i.e., exciton binding energy) is huge, on the order of 300−500 meV, relative to an energy gap of ∼1 eV.[24−27] As a result of this strong e−h attraction, it is generally accepted that the photoexcited state of a SWNT is excitonic (i.e., e−h pairs and no free electrons). In SWNTs, excitons are characterized by an e−h separation (Bohr radius) of approximately 2.5 nm.[24,26,28] Both the HOMO and LUMO levels of SWNTs are doubly degenerate, which gives rise to four degenerate singlet excitonic states. Coulomb interactions break this degeneracy, resulting in one allowed and three optically forbidden exciton states.[25,29] Because there is one optically active exciton per pair of matching peaks in the DOS, the linear absorptions and emissions of SWNTs approximate what would be observed from a simple free electron picture.

In summary, SWNTs experience quantum confinement due to their narrow circumference, creating unique electronic features that make nanotubes either metallic or semiconducting. Optical transitions take place between singularities in the DOS, but a more complete picture of the excited state must involve excitons. In this Account, we review several aspects of the photophysics of carbon nanotubes, including studies of

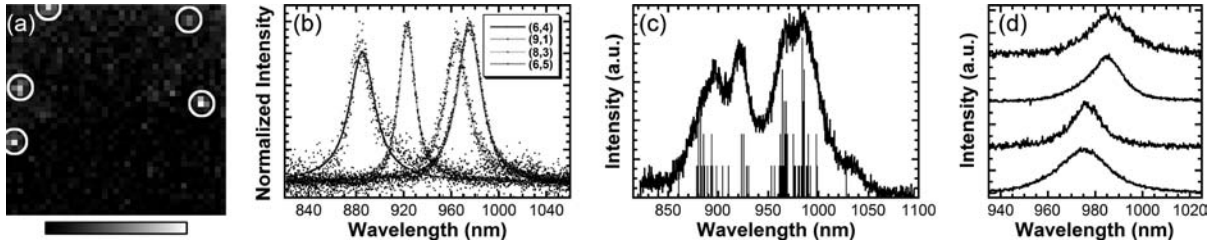

FIGURE 5. (a) Image (20 × 20 μm^2) of the fluorescence from single nanotubes (circled pixels). (b) Single-molecule fluorescence observed for four nanotube (*n*, *m*) structures. Spectra were integrated over 1 min, normalized, and fitted with Lorentzian functions. (c) Histogram of 77 single nanotubes overlaid with emission from an ensemble of SWNTs. (d) Fluorescence spectra for different single (6, 5) nanotubes, showing variation in peak position and line widths.

single nanotube fluorescence spectroscopy and excited-state exciton dynamics on ultrafast time scales.

Single Nanotube Spectroscopy

The important relationship between nanotube (*n*, *m*) structure and emission energy was first provided by ensemble fluorescence studies.[16] However, some key features such as line shapes and line widths were obscured by inhomogeneous line broadening and spectral overlap between fluorescence from different nanotube structures (Figure 4). In studies of single molecules, it is possible to determine these fundamental features directly and, perhaps, to observe additional unique behavior. For example, fluorescence intermittency (i.e., blinking) from single semiconductor quantum dots was discovered only by examining individual particles.[30]

For single-molecule measurements, nanotubes were dispersed into aqueous micellar suspensions[18] and spun cast onto quartz. Epifluorescence confocal microscopy enabled imaging of the emission from single nanotubes,[21] demonstrated in Figure 5a. Fluorescence intensity time traces, polarization curves, and Raman and fluorescence spectra were also recorded for individual SWNTs.[21] As the incident electric field (the polarized excitation) was rotated, the angular dependence of fluorescence intensity agreed very well with a $\cos^2 \theta$ dependence, as expected for a 1D molecule.[21,31]

Fluorescence spectra for individual nanotubes are displayed in Figure 5b. Individual SWNTs exhibit only one emission peak with an energy that approximately matches the corresponding (*n*, *m*) wavelength from the ensemble spectrum.[21] The observed fluorescence line shape is Lorentzian; interestingly, the full width at half-maximum is ~23 meV at room temperature, nearly equivalent to k_BT.[21] At low temperatures, line widths as narrow as 200 μeV are observed.[32] It is expected that the SWNT ensemble fluorescence spectrum can be reconstructed from a collection of single nanotube spectra, much like that observed for other single molecules such as CdSe quantum dots.[30] Figure 5c displays such a histogram for CoMoCAT-manufactured SWNTs, where again, the ensemble spectrum is completely recovered.

All SWNT carbon atoms lie on the molecule's surface,[33] and our laboratory was among the first to observe that the local environment significantly impacts nanotubes' optical spectra. For example, variations in peak position and line width are commonly observed for nanotubes of the same (*n*, *m*),[21] as shown for (6, 5) nanotubes in Figure 5d. The peak position can depend on defects in nanotubes' sidewalls introduced during their suspension[34] and upon the choice of surfactant used for solubilization.[19,35] Indeed, transition energies for surfactant-coated nanotubes are red-shifted by an average of ~28 meV compared with unprocessed SWNTs suspended across pillars,[36] or ~50 meV compared with as-grown SWNTs.[35] These shifts may result from screening of electron–hole interactions by the surrounding dielectric medium.[37]

SWNT fluorescence is also affected by other environmental factors. Temperature weakly influences the transition energy according to whether $(n - m) \bmod 3 = 1$ or 2.[38] For individual suspended SWNTs, the fluorescence red shifts with increasing temperature; for surfactant-isolated SWNTs, energy shifts are caused by the thermal expansion or contraction of the surfactant, which changes the pressure exerted on the nanotube.[39] Mechanical strain red or blue shifts the energy levels of the SWNT depending on the type of strain induced and the value of $(n - m) \bmod 3$.[40] A decrease in the optical transition energy accompanies an increase in the surrounding dielectric constant[37] or the application of a magnetic field.[41] Finally, spectral wandering is not observed at room temperature because the fluorescence line width is greater than the energy shift;[17] however, spectral diffusion up to 20 meV is observable at low temperature (4 K).[17,32]

Fluorescence intermittency, also known as on/off intensity blinking, is commonly used as the definitive indication that observed emission arises from an individual molecule. For example, under continuous excitation, the fluorescence from CdSe quantum dots cycles on and off at all times like a tele-

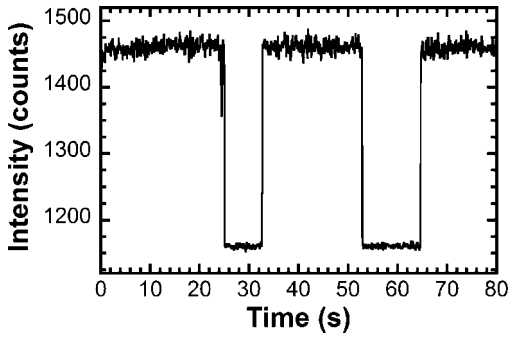

FIGURE 6. Single nanotube time trace. To show the contrast between on and off states for emission, the laser was physically blocked twice.

graph signal.[30] However, nanotubes' fluorescence emission surprisingly shows no indication of blinking on time scales ranging from 20 ms to 100 s (Figure 6). This absence of fluorescence blinking for single nanotubes is astonishing and distinguishes them from almost all other known emitters.[42] However, ~50% of emissive SWNTs exhibit blinking at low temperature (~1.8 K).[17] It is unclear whether blinking slows to an observable rate at low temperatures or blinking mechanisms become disabled at higher temperatures. For example, the trap and release of excitons at defect sites has been suggested as a plausible temperature-dependent blinking mechanism.[17]

Single-molecule fluorescence spectroscopy supplies a detailed and fundamental representation of the fluorescence properties of SWNTs, unencumbered by ensemble averaging effects. Important features of single nanotube emission include their Lorentzian line shapes, narrow k_BT-limited line widths, and the absence of blinking at room temperature. The local environment can strongly influence the optical transition energy of an individual SWNT.

Excited-State Dynamics

Time-resolved spectroscopies often provide a clearer picture of a molecule's fundamental electronic configuration than optical methods such as absorption, fluorescence, and resonant Raman spectroscopies. For example, time-resolved optical studies can determine radiative and nonradiative excited-state lifetimes, which are helpful for understanding fluorescence quantum yields. Time-resolved measurements for SWNTs are complemented by static electronic structure calculations,[26,43] time domain models of the SWNT response to strong laser pulses,[44,45] and simulations of electron–phonon relaxation.[46] For nanotubes, the excited-state relaxation dynamics should be significantly different for metallic and semiconducting SWNTs because these components feature inherently different electron energy states.

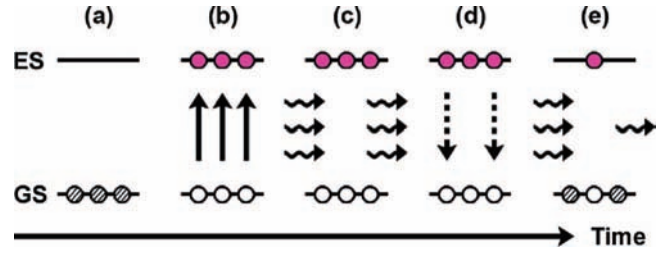

FIGURE 7. Illustration of one-color transient absorption: (a) A simple two-level system is assumed for illustrative purposes (GS is ground state and ES is excited state). (b) The pump pulse leaves the ground-state population depleted. (c) At a known time delay after the pump, a much weaker pulse (probe) is used to determine the transmittance. If the probe occurs immediately after the pump, excited molecules have not had time to relax. Thus, due to simple state-filling arguments (i.e., the ground state is depleted of electrons and the excited state is occupied, leaving less electrons to absorb), more of the probe intensity is transmitted. (d) As the probe is delayed further in time relative to the pump, more molecules have relaxed to the ground state. (e) Probe pulses are now more likely to be absorbed, and the transmission decreases.

We have focused on transient absorption (TA) spectroscopy to measure the excited-state relaxation dynamics of SWNTs.[47] As illustrated in Figure 7, a laser pulse (pump) places SWNTs into the excited state; a second delayed pulse (probe) is then used to monitor the population of a particular electronic state. As the excited-state population decays, any molecules that have returned to the ground state can absorb the probe pulse (excited molecules cannot), so the transmitted probe signal ($\Delta T/T$) decreases with time. This signal decay can be used to determine the depopulation dynamics of the excited state. In two-color TA spectroscopy, the pump and probe pulses have different energies, which is useful for monitoring spectrally resolved excited-state dynamics. For TA experiments, the pulse frequency (pulse widths ~150 fs) was tuned to be off- or on-resonance with respective E_{11} excitonic transitions of isolated nanotubes. For two-color studies, the E_{22} states of semiconducting SWNTs were populated and the E_{11} transitions for various (n, m) structures were monitored.

As anticipated for a quasi-two-level system, resonant excitation caused absorption saturation for all probe wavelengths, followed by an exponential decay of the signal with a time constant of ~220−420 fs. This decay was ascribed to relaxation through the continuum of electron levels in the conduction band for individual metal nanotubes or bundles of nanotubes.[47] Interestingly, when the probe was directly on-resonance with E_{11} transitions for semiconductor SWNTs, an additional slow decay component was observed (Figure 8a, lowest curve), but as the probe was tuned off-resonance, both the decay time and relative magnitude of this slow decay component decreased. Because the long decay component

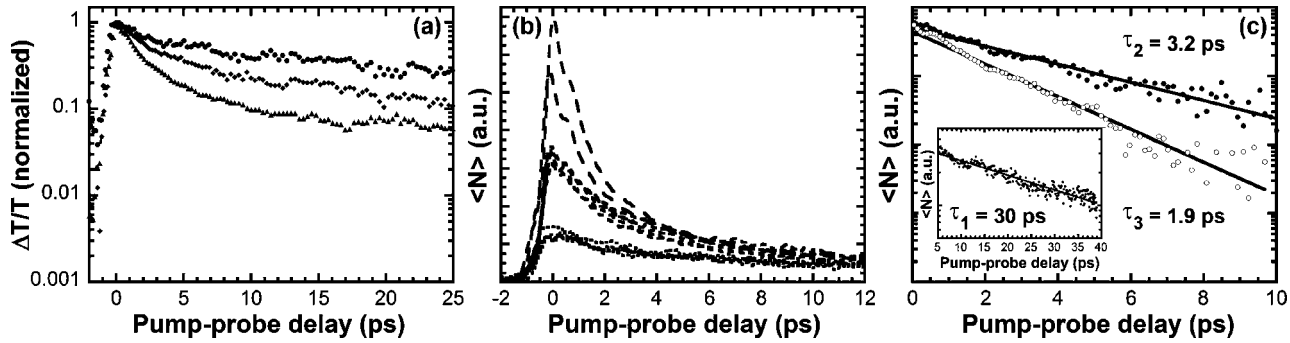

FIGURE 8. (a) Relative change in transmission for a probe wavelength of 1323 nm (pump wavelength is 800 nm). Three regimes of population decay are visible for each pump fluence (circles, diamonds, and triangles). (b) Quantized Auger response for increasing pump fluence, normalized at long decay times. (c) Extracted lifetime dynamics for one (inset), two (solid circles), and three (open circles) e−h pairs fit to a single-exponential decay.

coincided with on-resonance probe energies, this correlation suggests that carrier relaxation from the lowest semiconducting SWNT excitonic state caused this part of the response. Indeed, the lifetime of the slow decay component was ~120 ps, which agrees with lifetime estimates from FTIR photoluminescence ($\tau \approx 100$ ps)[48] and infrared time-correlated single-photon-counting spectroscopies ($\tau \approx 130$ ps).[49]

For excitons created at E_{22}, relaxation times into E_{11} were determined to be 20−110 fs.[50] These values agree with very fast relaxation times also found by Manzoni et al.[51] and theoretical predictions of subpicosecond decay from E_{22} to E_{11} performed by Habenicht et al.[46] As expected, longer recovery times were measured for SWNTs with E_{11} farther from the pump energy. This correlation strongly suggests that the excited-state dynamics studied here are the result of decay from e−h pairs that have relaxed to E_{11}. Further, the short excited-state lifetimes agree with measurements of a broad excited-state line width (35−70 meV) that is indicative of efficient inelastic exciton−phonon scattering.[52]

Quantized Auger Recombination

When a photoexcited electron and its hole recombine, the potential energy associated with this exciton can be emitted as a photon or it can be lost in a number of nonradiative processes. When multiple excitons are present, one of the most important nonradiative processes is Auger recombination (i.e., exciton−exciton annihilation), in which the energy released by the annihilated exciton is used to excite a second exciton to a higher energy level, as illustrated in Figure 9. Auger recombination requires that excitons occupy the same physical space and conserve momentum, which is difficult to achieve in macroscopic semiconductors. For nanometer-scale materials, Auger recombination is efficient because Coulomb (i.e., electrostatic) interactions are enhanced in confined systems and momentum conservation is relaxed, a result of the disruption in translation symmetry along the physically small nanoparticle.[53] Moreover, individual Auger recombination events become quantized due to the discrete number of excitons in a nanoparticle.[53]

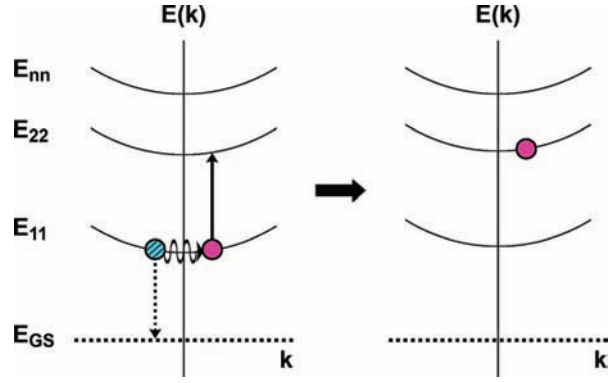

FIGURE 9. Diagram representing Auger recombination. The ground state (E_{GS}) and three nanotube exciton excited states (E_{11}, E_{22}, and E_{nn}) are shown. When the first exciton (blue, striped) decays, its energy is nonradiatively transferred to a second exciton (magenta, solid), which is promoted to a higher excited state.

For two-color TA studies, as the pump fluence was increased, the excited-state dynamics displayed three distinct signal recovery regimes, as illustrated in Figure 8a. As described earlier, the very fast (<500 fs) and relatively slow (~50−100 ps) signal recovery regimes were attributed to relaxation within the metallic nanotube conduction band and electron−hole recombination, respectively.[50] A region of moderately fast decay (2 ps ≤ probe delay ≤ 10 ps) was also present, and its decay rate was directly related to the pump fluence (i.e., relaxation became much faster as pump fluence increased).

Interestingly, as the pump intensity was increased, the TA spectra (normalized such that the signal magnitudes were equal at the longest decay) separated into three distinct bands, assigned to exciton recombination dynamics arising from one,

two, or three electron−hole pairs (Figure 8b).[50] The presence of quantized bands in the TA signal indicates quantized e−h recombination. Quantization arises because the number of excitons decreases discretely (i.e., three to two to one e−h pair) and each state has a characteristic lifetime.[53] The first cluster of curves corresponds to excited-state dynamics of SWNTs excited with only one e−h pair. The next two groups were assigned to SWNTs containing two e−h pairs (middle group) and three e−h pairs (top group).

We found that the TA curves corresponding to one, two, and three electron−hole pairs are simple linear combinations of one, two, and three exponential functions, respectively, so an iterative subtractive procedure was used to recover the lifetime for each separate process, τ_N.[50,53,54] These extracted dynamics are presented in Figure 8c. The lifetimes of the two e−h and three e−h pair states ($\tau_2 \approx 3$ ps and $\tau_3 \approx 2$ ps, respectively) indicate that the Auger response is relatively very strong in SWNTs. For comparison, in CdSe quantum dots and quantum rods, τ_2 and τ_3 are on the order of tens to hundreds of picoseconds. The strong Auger response indicates a large e−h Coulomb interaction that is consistent with the enormous SWNT exciton binding energy.[25]

The ratio of τ_2/τ_3 elucidates whether free carriers or excitons better describe the excited state. Free carrier Auger processes involve three quasi-particles (i.e., electron, hole, and third charge carrier), but excitonic Auger processes involve only two particles (i.e., two excitons).[53] The difference in the underlying nature of the Auger process for free electrons versus excitons leads to a different dependence of the ratio τ_2/τ_3: $\tau_2/\tau_3 \approx 2.25$ for free carriers and $\tau_2/\tau_3 \approx 1.5$ for excitons.[54] Thus, the ratio of τ_2/τ_3 can provide strong evidence about the nature of the SWNT excited state. For photoexcited SWNTs, the value of τ_2/τ_3 was ~1.5, and thus, the exciton excited-state picture is directly and clearly supported by these TA studies.[50]

In summary, ultrafast TA measurements complement single-molecule studies and have been used to clarify the time scale and nature of ground-state recovery in nanotubes and to extract excitonic lifetime information. For relaxation from the excited state, the ever-present fast decay component ($\tau \approx$ 300−500 fs) likely is due to SWNT bundles and metallic nanotubes; however, the much slower decay component ($\tau \approx$ 50−100 ps) only appears when probing on-resonance for a semiconductor SWNT and likely corresponds to the excited-state lifetime of the photoexcited exciton. Further, the rapid quantized exciton annihilation response at high pump fluences confirms that excitons are responsible for the optical resonances in carbon nanotubes.

Outlook and Future Direction

Nearly a decade and a half after their discovery,[55] carbon nanotubes continue to fascinate the scientific community. As described in this Account, SWNTs possess several unique photophysical features that arise from their interesting molecular structure and small radial dimensions. As the photophysical properties of carbon nanotubes become better understood, emphasis will shift toward whether these unqiue properties could enable ground-breaking applications.

SWNTs may satisfy a long-standing need for superior florophores for *in vivo* single biomolecule imaging and tracking. Most known fluorophores suffer from photoinduced bleaching, but strikingly, nanotubes' emission remains steady, even over hours of continuous excitation.[21,56] Coupled with their relative ease of uptake into cells and infrared emission at wavelengths most transparent to biological tissue, SWNTs have great promise in this area.[3,4,56]

Stable near-infrared fluorescence also makes carbon nanotubes exciting candidates for single-photon sources. For example, quantum cryptography requires a single-photon source because those that emit two or more photons provide opportunities for a compromised transmission.[57] SWNTs are an excellent single-photon source because they do not show fluorescence intermittency, nor do they photobleach.[17]

Still, many areas of nanotube photophysics pose important questions. For example, the measured line widths and photoluminescent lifetimes of SWNTs depend strongly on the local environment in an unknown manner.[58,59] Similarly, it is unclear what causes the majority of nanotubes to have an extremely low fluorescence quantum yield. For different (n, m) structures, the tight binding model predicts optical transition energies that are so much smaller than observed energies that controversy surrounds why this model works at all.[24−26,60] The recent prediction of a forbidden exciton state, the energy of which is below that of the allowed exciton, may also play a large role in SWNT optical properties.[25,61] Continuing efforts to understand the remarkable photophysical properties of carbon nanotubes are essential to the realization and success of applications based on these materials.

We thank the following for their financial support: the Camille and Henry Dreyfus Foundation, the Sloan Foundation, and the Department of Energy Office of Basic Energy Sciences.

BIOGRAPHICAL INFORMATION

Lisa J. Carlson grew up in Eden, NY, and completed her B.S. in Chemistry and Secondary Education at the State University of New York at Fredonia in 2004. She earned her M.S. in Chemis-

try in 2006 from the University of Rochester, where she is currently working toward her Ph.D. with Todd Krauss. As part of her graduate research, Lisa uses single-molecule spectroscopy to investigate fundamental optical properties of carbon nanotubes.

Todd D. Krauss is an Associate Professor of Chemistry at the University of Rochester. He received his B.S., M.S., and Ph.D. all from Cornell University, the latter under the advisement of Frank Wise. Upon graduating in 1998, he moved to Columbia University, serving as a postdoctoral fellow under Louis Brus until 2000, when he joined the Chemistry faculty at the University of Rochester as an Assistant Professor. Krauss's research interests involve fundamental studies of materials at the nanometer scale, down to the single-molecule level, with a specific emphasis on single-walled carbon nanotubes and semiconductor quantum dots. In addition, he is pursuing applications for these nanometer scale materials in the general areas of novel biological sensors and nanophotonics.

FOOTNOTES

*To whom correspondence should be addressed. E-mail: krauss@chem.rochester.edu.

REFERENCES

1 Collins, P. G.; Avouris, P. Nanotubes for electronics. *Sci. Am.* **2000**, 62–69.

2 Wong, S. S.; Harper, J. D.; Lansbury, P. T.; Lieber, C. M. Carbon nanotube tips: High-resolution probes for imaging biological systems. *J. Am. Chem. Soc.* **1998**, *120*, 603–604.

3 Barone, P. W.; Parker, R. S.; Strano, M. S. In vivo fluorescence detection of glucose using a single-walled carbon nanotube optical sensor: Design, fluorophore properties, advantages, and disadvantages. *Anal. Chem.* **2005**, *77*, 7556–7562.

4 Cherukuri, P.; Gannon, C. J.; Leeuw, T. K.; Schmidt, H. K.; Smalley, R. E.; Curley, S. A.; Weisman, R. B. Mammalian pharmacokinetics of carbon nanotubes using intrinsic near-infrared fluorescence. *Proc. Natl. Acad. Sci. U.S.A.* **2006**, *103*, 18882–18886.

5 Heller, D. A.; Baik, S.; Eurell, T. E.; Strano, M. S. Single-walled carbon nanotube spectroscopy in live cells: Towards long-term labels and optical sensors. *Adv. Mater.* **2005**, *17*, 2793–2799.

6 Chen, J.; Perebeinos, V.; Freitag, M.; Tsang, J.; Fu, Q.; Liu, J.; Avouris, P. Bright infrared emission from electrically induced excitons in carbon nanotubes. *Science* **2005**, *310*, 1171–1174.

7 Liu, C.; Fan, Y. Y.; Liu, M.; Cong, H. T.; Cheng, H. M.; Dresselhaus, M. S. Hydrogen storage in single-walled carbon nanotubes at room temperature. *Science* **1999**, *286*, 1127–1129.

8 Park, J.; McEuen, P. L. Formation of a p-type quantum dot at the end of an n-type carbon nanotube. *Appl. Phys. Lett.* **2001**, *79*, 1363–1365.

9 Derycke, V.; Martel, R.; Appenzeller, J.; Avouris, P. Carbon nanotube inter- and intramolecular logic gates. *Nano Lett.* **2001**, *1*, 453–456.

10 Postma, H. W. C.; Teepen, T.; Yao, Z.; Grifoni, M.; Dekker, C. Carbon nanotube single-electron transistors at room temperature. *Science* **2001**, *293*, 76–79.

11 Rueckes, T.; Kim, K.; Joselevich, E.; Tseng, G. Y.; Cheung, C.-L.; Lieber, C. M. Carbon nanotube-based nonvolatile random access memory for molecular computing. *Science* **2000**, *289*, 94–97.

12 Martel, R.; Schmidt, T.; Shea, H. R.; Hertel, T.; Avouris, P. Single- and multi-wall carbon nanotube field-effect transistors. *Appl. Phys. Lett.* **1998**, *73*, 2447–2449.

13 Saito, R.; Dresselhaus, G.; Dresselhaus, M. S. *Physical Properties of Carbon Nanotubes*, 1st ed.; Imperial College Press: London, 1998.

14 Hagen, A.; Hertel, T. Quantitative analysis of optical spectra from individual single-wall carbon nanotubes. *Nano Lett.* **2003**, *3*, 383–388.

15 Dresselhaus, M. S.; Dresselhaus, G.; Jorio, A.; Souza Filho, A. G.; Pimenta, M. A.; Saito, R. Single nanotube Raman spectroscopy. *Acc. Chem. Res.* **2002**, *35*, 1070–1078.

16 Bachilo, S. M.; Strano, M. S.; Kittrell, C.; Hauge, R. H.; Smalley, R. E.; Weisman, R. B. Structure-assigned optical spectra of single-walled carbon nanotubes. *Science* **2002**, *298*, 2361–2366.

17 Hartschuh, A.; Pedrosa, H. N.; Peterson, J.; Huang, L.; Anger, P.; Qian, H.; Meixner, A. J.; Steiner, M.; Novotny, L.; Krauss, T. D. Single carbon nanotube optical spectroscopy. *ChemPhysChem* **2005**, *6*, 577–582.

18 O'Connell, M. J.; Bachilo, S. M.; Huffman, C. B.; Moore, V. C.; Strano, M. S.; Haroz, E. H.; Rialon, K. L.; Boul, P. J.; Noon, W. H.; Kitrell, C.; Ma, J.; Hauge, R. H.; Weisman, R. B.; Smalley, R. E. Band gap fluorescence from individual single-walled carbon nanotubes. *Science* **2002**, *297*, 593–596.

19 Moore, V. C.; Strano, M. S.; Haroz, E. H.; Hauge, R. H.; Smalley, R. E.; Schmidt, J.; Talmon, Y. Individually suspended single-walled carbon nanotubes in various surfactants. *Nano Lett.* **2003**, *3*, 1379–1382.

20 Zheng, M.; Jagota, A.; Strano, M. S.; Santos, A. P.; Barone, P.; Chou, S. G.; Diner, B. A.; Dresselhaus, M. S.; Mclean, R. S.; Onoa, G. B.; Samsonidze, G. G.; Semke, E. D.; Usrey, M.; Walls, D. J. Structure-based carbon nanotube sorting by sequence-dependent DNA assembly. *Science* **2003**, *302*, 1545–1548.

21 Hartschuh, A.; Pedrosa, H. N.; Novotny, L.; Krauss, T. D. Simultaneous fluorescence and Raman scattering from single carbon nanotubes. *Science* **2003**, *301*, 1354–1356.

22 Kataura, H.; Kumazawa, Y.; Maniwa, Y.; Umezu, I.; Suzuki, S.; Ohtsuka, Y.; Achiba, Y. Optical properties of single-wall carbon nanotubes. *Synth. Mater.* **1999**, *103*, 2555–2558.

23 Weisman, R. B.; Bachilo, S. M. Dependence of optical transition energies on structure for single-walled carbon nanotubes in aqueous suspension: An empirical Kataura plot. *Nano Lett.* **2003**, *3*, 1235–1238.

24 Perebeinos, V.; Tersoff, J.; Avouris, P. Scaling of excitons in carbon nanotubes. *Phys. Rev. Lett.* **2004**, *92*, 257402.

25 Zhao, H.; Mazumdar, S. Electron-electron interaction effects on the optical excitations of semiconducting single-walled carbon nanotubes. *Phys. Rev. Lett.* **2004**, *93*, 157402.

26 Spataru, C. D.; Ismail-Beigi, S.; Benedict, L. X.; Louie, S. G. Excitonic effects and optical spectra of single-walled carbon nanotubes. *Phys. Rev. Lett.* **2004**, *92*, 077402.

27 Wang, Z.; Zhao, H.; Mazumdar, S. Quantitative calculations of the excitonic energy spectra of semiconducting single-walled carbon nanotubes within a π-electron model. *Phys. Rev. B* **2006**, *74*, 195406.

28 Wang, F.; Dukovic, G.; Brus, L. E.; Heinz, T. F. The optical resonances in carbon nanotubes arise from excitons. *Science* **2005**, *308*, 838–841.

29 Perebeinos, V.; Tersoff, J.; Avouris, P. Radiative lifetime of excitons in carbon nanotubes. *Nano Lett.* **2005**, *5*, 2495–2499.

30 Nirmal, M.; Dabbousi, B. O.; Bawendi, M. G.; Macklin, J. J.; Trautman, J. K.; Harris, T. D.; Brus, L. E. Fluorescence intermittency in single cadmium selenide nanocrystals. *Nature* **1996**, *383*, 802–804.

31 Islam, M. F.; Milkie, D. E.; Kane, C. L.; Yodh, A. G.; Kikkawa, J. M. Direct measurement of the polarized optical absorption cross section of single-wall carbon nanotubes. *Phys. Rev. Lett.* **2004**, *93*, 037404.

32 Htoon, H.; O'Connell, M. J.; Cox, P. J.; Doorn, S. K.; Klimov, V. I. Low temperature emission spectra of individual single-walled carbon nanotubes: Multiplicity of subspecies within single-species nanotube ensembles. *Phys. Rev. Lett.* **2004**, *93*, 027401.

33 Lefebvre, J.; Homma, Y.; Finnie, P. Bright band gap photoluminescence from unprocessed single-walled carbon nanotubes. *Phys. Rev. Lett.* **2003**, *90*, 217401.

34 Heller, D. A.; Barone, P. W.; Strano, M. S. Sonication-induced changes in chiral distribution: A complication in the use of single-walled carbon nanotube fluorescence for determining species distribution. *Carbon* **2005**, *43*, 651–653.

35 Okazaki, T.; Saito, T.; Matsuura, K.; Ohshima, S.; Yumura, M.; Iijima, S. Photoluminescence mapping of "as-grown" single-walled carbon nanotubes: A comparison with micelle-encapsulated nanotube solutions. *Nano Lett.* **2005**, *5*, 2618–2623.

36 Lefebvre, J.; Fraser, J. M.; Homma, Y.; Finnie, P. Photoluminescence from single-walled carbon nanotubes: A comparison between suspended and micelle-encapsulated nanotubes. *Appl. Phys. A: Mater. Sci. Process.* **2004**, *78*, 1107–1110.

37 Walsh, A. G.; Vamivakas, A. N.; Yin, Y.; Cronin, S. B.; Ünlü, M. S.; Goldberg, B. B.; Swan, A. K. Screening of excitons in single, suspended carbon nanotubes. *Nano Lett.* **2007**, *7*, 1485–1488.

38 Capaz, R. B.; Spataru, C. D.; Tangney, P.; Cohen, M. L.; Louie, S. G. Temperature dependence of the band gap of semiconducting carbon nanotubes. *Phys. Rev. Lett.* **2005**, *94*, 036801.

39 Cronin, S. B.; Yin, Y.; Walsh, A.; Capaz, R. B.; Stolyarov, A.; Tangney, P.; Cohen, M. L.; Louie, S. G.; Swan, A. K.; Ünlü, M. S.; Goldberg, B. B.; Tinkham, M. Temperature dependence of the optical transition energies of carbon nanotubes: The role of electron-phonon coupling and thermal expansion. *Phys. Rev. Lett.* **2006**, *96*, 127403.

40 Shan, G.; Bao, S. The effect of deformations on electronic structures and optical properties of carbon nanotubes. *Physica E* **2006**, *35*, 161–167.

41 Zaric, S.; Ostojic, G. N.; Kono, J.; Shaver, J.; Moore, V. C.; Strano, M. S.; Hauge, R. H.; Smalley, R. E.; Wei, X. Optical signatures of the Aharonov-Bohm phase in single-walled carbon nanotubes. *Science* **2004**, *304*, 1129–1131.

42 Trautman, J. K.; Macklin, J. J.; Brus, L. E.; Betzig, E. Near-field spectroscopy of single molecules at room temperature. *Nature* **1994**, *369*, 40–42.

43 Barone, V.; Peralta, J. E.; Wert, M.; Heyd, M.; Scuseria, G. E. Density functional theory study of optical transitions in semiconducting single-walled carbon nanotubes. *Nano Lett.* **2005**, *5*, 1621–1624.

44 Romero, A. H.; Garcia, M. E.; Valencia, F.; Terrones, H.; Terrones, M.; Jeschke, H. O. Femtosecond laser nanosurgery of defects in carbon nanotubes. *Nano Lett.* **2005**, *5*, 1361–1365.

45 Dumitrica, T.; Garcia, M. E.; Jeschke, H. O.; Yakobson, B. I. Selective cap opening in carbon nanotubes driven by laser-induced coherent phonons. *Phys. Rev. Lett.* **2004**, *92*, 117401.

46 Habenicht, B. F.; Craig, C. F.; Prezhdo, O. V. Time-domain ab initio simulation of electron and hole relaxation dynamics in a single-wall semiconducting carbon nanotube. *Phys. Rev. Lett.* **2006**, *96*, 187401.

47 Huang, L.; Pedrosa, H. N.; Krauss, T. D. Ultrafast ground-state recovery of single-walled carbon nanotubes. *Phys. Rev. Lett.* **2004**, *93*, 017403.

48 Lebedkin, S.; Arnold, K., Hennrich, F., Krupke, R., Renker, B. Kappes, M. M., Photoluminescence of single-walled carbon nanotubes: Estimate of the lifetime and FTIR-luminescence mapping. In *Molecular Nanostructures*, Proceedings of the AIP Conference; Kuzmany, H.; Fink, J., Mehring, M., Roth, R., Eds.; AIP: New York, **2003**; *685*, p. 230.

49 Jones, M.; Engtrakul, C.; Metzger, W. K.; Ellingson, R. J.; Nozik, A. J.; Heben, M. J.; Rumbles, G. Analysis of photoluminescence from solubilized single-walled carbon nanotubes. *Phys. Rev. B* **2005**, *71*, 115426.

50 Huang, L.; Krauss, T. D. Quantized bimolecular Auger recombination of excitons in single-walled carbon nanotubes. *Phys. Rev. Lett.* **2006**, *96*, 057407.

51 Manzoni, C.; Gambetta, A.; Menna, E.; Meneghetti, M.; Lanzani, G.; Cerullo, G. Intersubband exciton relaxation dynamics in single-walled carbon nanotubes. *Phys. Rev. Lett.* **2005**, *94*, 207401.

52 Htoon, H.; O'Connell, M. J.; Doorn, S. K.; Klimov, V. I. Single carbon nanotubes probed by photoluminescence excitation spectroscopy: The role of phonon-assisted transitions. *Phys. Rev. Lett.* **2005**, *94*, 127403.

53 Klimov, V. I.; Mikhailovsky, A. A.; McBranch, D. W.; Leatherdale, C. A.; Bawendi, M. G. Quantization of multiparticle Auger rates in semiconductor quantum dots. *Science* **2000**, *287*, 1011–1013.

54 Htoon, H.; Hollingsworth, J. A.; Dickerson, R.; Klimov, V. I. Effect of zero- to one-dimensional transformation on multiparticle Auger recombination in semiconductor quantum rods. *Phys. Rev. Lett.* **2003**, *91*, 227401.

55 Iijima, S. Helical microtubules of graphitic carbon. *Nature* **1991**, *354*, 56–58.

56 Barone, P. W.; Baik, S.; Heller, D. A.; Strano, M. S. Near-infrared optical sensors based on single-walled carbon nanotubes. *Nat. Mater.* **2004**, *4*, 86–92.

57 Lounis, B.; Moerner, W. E. Single photons on demand from a single molecule at room temperature. *Nature* **2000**, *407*, 491–493.

58 Hagen, A.; Steiner, M.; Raschke, M. B.; Lienau, C.; Hertel, T.; Qian, H.; Meixner, A. J.; Hartschuh, A. Exponential decay lifetimes of excitons in individual single-walled carbon nanotubes. *Phys. Rev. Lett.* **2005**, *95*, 197401.

59 Wang, F.; Dukovic, G.; Brus, L. E.; Heinz, T. F. Time-resolved fluorescence of carbon nanotubes and its implication for radiative lifetimes. *Phys. Rev. Lett.* **2004**, *92*, 177401.

60 Perebeinos, V.; Tersoff, J.; Avouris, P. Effect of exciton-phonon coupling in the calculated optical absorption of carbon nanotubes. *Phys. Rev. Lett.* **2005**, *94*, 027402.

61 Spataru, C. D.; Ismail-Beigi, S.; Capaz, R. B.; Louie, S. G. Theory and ab initio calculation of radiative lifetimes of excitons in semiconducting carbon nanotubes. *Phys. Rev. Lett.* **2005**, *95*, 247402.